LRIS Astrometry As Of April 2007

Judith G. Cohen and Wenjin Huang – Caltech – August 2007

ABSTRACT

In this document we present fits for the distortion of the LRIS-R and LRIS-B instrument focal plane applicable to the determination of astrometric coordinates from imaeges taken with the LRIS at the Keck I Telescope. Coefficients were determined for LRIS-R and LRIS-B with the ADC in use and without the ADC in the beam based on images taken in the time period Jan. to March, 2007. These are utilized in the latest version (version 3.0) of the program COORDINATES.

The last section contains for warnings regarding the various instrumental configurations of LRIS, the epochs at which astrometric fits for LRIS were carried out, and other relevant issues.

1. Introduction and Motivation

The first complete analysis of LRIS astrometry is described in the report "The Spatial Distortion in the LRIS" by J.Cohen from Dec. 1994, and most recent such analysis is given in "The Spatial Distortion in the LRIS – Addendum 5" by J. Cohen and P. Shopbell from Nov. 1996. This was before the installation of LRIS-B, so a detailed study of the LRIS astrometry is long overdue.

The motivation for such a study at the present time is the commissioning of the atmospheric dispersion compensator (ADC), which corrects the image of a star to be a point even when it is not at the zenith by compensating for atmospheric dispersion. This minimizes light loss at the slit for spectroscopy and eliminates the need to observe at the parallactic angle. Observing at the parallactic angle is often not feasible for slitmasks, which must be used at a fixed position angle defined at the time they are designed. Present practice is to guess the hour angle at which the slit mask will be used and apply an appropriate correction for atmospheric dispersion to the object positions. However, given the wide spectral coverage of the dual-beam LRIS from the near UV to 1μ, that will not keep the spectra aligned with the slit unless the field of interest at the time of observation is near the zenith or the guess for the hour angle of use is close to correct and the exposure is short.

Light loss at the entrance slit of LRIS, particularly in the UV where atmospheric dispersion is large even at modest zenith angles, is minimized by the use of the ADC. We expect

use of the ADC to become the default mode of observing with LRIS now that it has been commissioned. Since the ADC contains a pair of counter-rotating prisms of small but not ignorable optical thickness, it introduces a small change into the scale of the LRIS at the detector focal plane.

2. LRIS Red and Blue Detector Formats

LRIS images are read out and saved as FITS files.

The LRIS red side has a single Tektronix 2048x2048 CCD with 24 μ pixels. It is read out by two amplifiers with slightly different electronic characteristics, so the frames have a discontinuity in bias level in the center, but the detector is a single CCD. Note that Keck plans to replace this detector within a year or two.

Throughout this document we use X, Y coordinates as indicated via cursor readout with the image display server ds9 operating on the standard FITS files generated by LRIS at the Keck I telescope. A LRIS-R FITS image begins with 40 columns of bias data (20 for each of the two amplifiers). Thus pixel 1,1 in a LRIS-R frame falls within the regime of bias values. The detector pixels cover the regime $X = 41 - 2088$, $Y = 1 - 2048$. There are then additional bias columns read out and stored after the last of the actual detector pixels has been read out. The center of the detector is at $X, Y = 1064, 1024$ on the FITS image. The illuminated area for direct imaging with LRIS-R extends in X approximately from pixels 150 to 1790, and in Y over the full height of the CCD, pixels 1–2048.

LRIS-B has a detector which is a mosaic of two 2048x4096 pixel CCDs. Each pixel is 15 μ on a side. These detectors are read out and the two separate images are assembled into a single FITS file which is 4620 x 4096 pixels. In the detector readout configuration in use in early 2007, the first 204 columns are bias values, the actual image covers $X = 205 - 4300$, $Y = 1 - 4096$, then additional bias columns are saved at $X > 4300$ pixels. The two CCDs thus cover $X = 205 - 2252$ (the left CCD in the final image) and $X = 2253 - 4300$ (the right CCD), with both extending over $Y = 1, 4096$. The LRIS-B detector produces images which are rotated by 90° with respect to LRIS-R image.

The program COORDINATES allows you to obtain accurate RA and Dec coordinates for objects on direct images taken with the Low Resolution Imaging Spectrograph (LRIS) at the Keck Observatory from a list of their X, Y positions on the LRIS blue or red detector.

The help document for COORDINATES explains in detail how to use this program, how to set up the input file, etc. Here we deal only with the derivation of the astrometric

fits used within this program.

The present update of COORDINATES implements the distortion fits derived here for LRIS–B and LRIS–R with and without the ADC, and is based on images taken between Dec 2006 and March 2007. Fig. 1 illustrates the distortion pattern from a linear fit for the LRIS-R focal plane.

Please be sure to read the last section of this report for warnings regarding the various instrumental configurations of LRIS, the epochs at which astrometric fits for LRIS were carried out, and related issues.

3. Details of Analysis Procedure

Images of fields with accurate astrometry have been used to determine the distortion pattern of the focal plane for each of the cameras (red and blue) of LRIS. The variables input into program COORDINATES are X, Y(CCD) and, if available, RA,Dec for reference stars. The input X, Y(CCD) include any pre-image readouts or preline readouts whose pixels are virtual and do not exist as physical pixels on the LRIS detectors. Such virtual pixels are used to determine bias levels or other electronic properties of the readout circuitry. Internal to the fitting process described below we use physical pixels on the LRIS detectors. We do this to avoid having to modify the fits if a change is made to the parameters affecting the readout, the number of CCD amplifiers used, etc. Thus the first step in determining any fit is to remove the prepix and preline pixels so that X, Y(CCD)(1,1) corresponds to the lower left corner pixel as viewed in ds9 which is actually on the detector itself. RA and Dec are expressed internally in program COORDINATES as offsets in arcsec from the center of the imaged field.

We use a third order polynomial fit in X and in Y, so each fit has 10 coefficients, $A(1)$ to $A(10)$, for X and coefficients $B(1)$ to $B(10)$ for Y. These coefficients have been determined by fitting the known coordinates of stars versus their position in the LRIS focal plane CCD detector for each of of LRIS-B and LRIS-R.

The form of the polynomial is:

$$X(SKY) = A(1) + A(2) * xin + A(3) * yin + A(4) * xin^2 + A(5) * yin^2 + A(6) * xin * yin$$
$$+A(7) * (xin^3) + A(8) * xin^2 * yin + A(9) * xin * yin^2 + A(10) * yin^3$$

xin and yin are the X, Y pixels in the CCD image from LRIS. $X(SKY)$ and $Y(SKY)$ are

the offsets in arcsec from the center of the field, with the atmospheric refraction removed. The center of the field is assumed to be the center of rotation when the position angle is not 0. At PA = 0°, following normal astronomical conventions, $-X(SKY)$ is East and $+Y(SKY)$ is North.

We use images of the open cluster NGC 2158 to determine the coefficients. K. Cudworth (private communication) supplied to us in 1989 astrometric coordinates with uncertainties of 0.1 arcsec in each of RA and Dec for more than 1000 stars in this cluster within a field larger than the full LRIS field (roughly 6x8 arcmin). He measured photographic plates to determine the positions of stars in the field of NGC 2158. They have an epoch of about 1960. The ∼50 year time to the present means that proper motion differences between cluster members and non-members or high proper motion objects may be detectable.

Images of the field of NGC 2158 were taken with and without the ADC in the beam. Filters used were V and R for the red side, and B and g for the blue side. Since the stars are bright, 1 second exposures were used.

About 740 of these stars appear within a single LRIS image of NGC 2158. The X, Y positions of these stars were measured on each image. The next step is to determine the position angle of the image. We select the stars close to the center of the field (within a radius of 350 pixels of the center for LRIS-R images), and carry out a linear fit to this group of stars (about 105 stars for the NGC 2158 images). The position angle is determined from the coefficients $A(2)$, $A(3)$, $B(2)$ and $B(3)$.

Then we determine the exact RA,Dec corresponding to the center of the field. If the telescope pointing were perfect, which is not generally the case, this would correspond to the coordinates in the FITS headers. The RA,Dec of the field center is found by guessing the coordinates of the center, proceeding through the linear fit including only stars near the center, and looking the pixel coordinates X, Y(CCD) corresponding to $X(SKY) = Y(SKY) = 0$. The difference is used to inform a better second guess for the RA,Dec of the center of the field. When those correspond to the the center of LRIS detector, the RA,Dec for the center is correct. With experience, this process can be carried out successfully in only two iterations.

Once the RA,Dec for the center of the field and the position angle of the image are known, we rotate the set of RA,Dec coordinates, converted into arcsec offsets from the central RA,Dec, so that they are correct for PA = 0. We then carry out the third order fit, minimizing the residuals. Note that we are free to rotate the coordinates on the sky, but cannot rotate those measured on the LRIS CCD detector.

Additional images with and without the ADC were obtained by A. Phillips of a field in Leo I. The coordinates of stars in this field used to analyze the astrometry of LRIS are from

Peter Stetson's on-line database (see Stetson, 2000, PASP, 112, 925). The precision of this astrometry may not be not as high as that of K. Cudworth's astrometry and the number of stars within the field of LRIS included in Stetson's table is only ∼300, less than half of the number for the NGC 2158 fields. However, the proper motion issue is greatly alleviated as these coordinates are based on recent CCD imaging. We have used the Leo I images to verify the validity of the astrometric fits. The stars of interest are fainter in this field; typical exposure times were 300 sec.

Relevant data for the images used here is given in Table 1.

Frame	Field	Date	ADC	Filter	Star#
lred0040	NGC2158	2007/01/28	Yes	R	746
lred0041	NGC2158	2007/01/28	Yes	V	728
lred0052	Leo I	2007/01/28	Yes	R	285
lred0070	NGC2158	2007/02/16	No	R	751
lred0071	NGC2158	2007/02/16	No	R	747
lred0102	Leo I	2007/03/09	Yes	R	289
lred0250	Leo I	2006/12/29	No	R	278
lblue0055	NGC2158	2007/01/28	Yes	g	697
lblue0056	NGC2158	2007/01/28	Yes	B	667
lblue0062	NGC2158	2007/02/16	No	B	727
lblue0063	NGC2158	2007/02/16	No	B	723
lblue0096	Leo I	2007/01/28	Yes	B	319
lblue0162	Leo I	2007/03/09	Yes	g	316
lblue0205	Leo I	2006/12/29	No	B	298

Table 1: Information for All Images Used in This Report

4. The Red Camera: LRIS–R

The situation for the red side of LRIS is straightforward. The resulting 10 coefficients for each of X and Y with and without the ADC installed are given below. The predicted change in scale from the optical design of the ADC (ADC PDR Optics Report, Section 7) was a factor of 0.99857 (in the sense that arcsec per pixel increases). The value we measured from LRIS-R images is 0.9985, in excellent agreement with the predictions.

The updated coefficients for the astrometric fits to LRIS-R images are given in Table 2. Image lred0040 was used for the case of the ADC in, while lred0070 was used for the ADC

out case. These coefficients will give offsets in arcsec in X and in Y from the center of the field in a coordinate system where the center of the imaging field (i.e. the axis of rotation for position angle) is pixel 1024, 1024. If the position angle of the image is 0°, then $-X$ is East and $+Y$ is North.

X/Y	ADC	1	x	y	x^2
		y^2	xy	x^3	x^2y
		xy^2	y^3		
lred0040					
X	Yes	215.39475	−0.20950212	0.30710551E−02	−0.20525413E−05
		−0.14337209E−05	−0.21997301E−05	0.77741210E−09	−0.17289732E−10
		0.11033589E−08	−0.57206933E−10		
Y	Yes	−216.10848	−0.11223419E−02	0.20869838	0.11890912E−05
		0.33875056E−05	0.10158390E−05	−0.57186568E−10	−0.10449538E−08
		0.48144598E−10	−0.11278520E−08		
lred0070					
X	No	214.83418	−0.20825571	0.32599909E−02	−0.30204635E−05
		−0.15392512E−05	−0.23929830E−05	0.10442439E−08	0.11155732E−09
		0.10654012E−08	−0.14505548E−10		
Y	No	−215.68238	−0.11120534E−02	0.20829835	0.11878170E−05
		0.32459433E−05	0.11281612E−05	−0.68787117E−10	−0.10104519E−08
		−0.70793360E−11	−0.10475806E−08		

Table 2: Coefficients for LRIS-R (Third Order Polynomial Fit)

We can address several issues at this point. The first is how accurately the LRIS image rotator performs. We have determined the correct position angle of each image, and we can compare that to the position angle of the telescope (keyword ROTPOSN in the image header). Table 3 gives the results.

This table is puzzling. In the past, typical PA errors were in the range −0.15 to 0.15 deg. The value of −0.9 deg for one of the Leo I images (frame lred0250) is disturbingly large. It has been verified through the use of multiple independent codes by both J. Cohen and W. Huang.

The frames analyzed here cover a four month interval. While this is short compared to the interval of several years for the set of images utilized in earlier work on the LRIS astrometry by J. Cohen, we proceed to examine the stability with time by looking at the

residuals after applying the fits for LRIS-R given in Table 2. We divide each image into 9 equal area sectors, with sector 1 being the upper left (X small, Y large), sector 5 being the middle, and sector 9 the lower right (X large, Y small) of the image. There are enough stars in each sector to determine the rms residuals in X and in Y when the fits are applied to each frame. Table 4 lists the rms position error ($\sqrt{\sigma_x^2 + \sigma_y^2}$) for each sector for the available images. The values are in arcsec.

We see that applying the third order fits in X and in Y to the image from which it was derived leads to 2D residuals of 0.08 arcsec over the entire area of the image. This is comparable to the uncertainty of the input RA,Dec for the stars in NGC 2158.

When a fit is applied to images other than the one from which it was derived, the 2D residuals are small in the central region of an image, but increase up to 0.2 arcsec at the edge of the field for images taken on a different run. This is illustrated in Fig. 4 and in Fig. 5. The distortion pattern is not a rotation, rather its closer to a pincushion distortion.

The maximum 2D deviation seen in this study, even when a fit from LRIS-R image A is applied to image B, is 0.30 arcsec. Such a large value is seen for only one of the comparisons listed in Table 4 and occurs only in the lower right sector (i.e. one of the corners of the LRIS field) of that image.

The crucial value for slitmasks is the 1D residuals in the direction along the width of the narrow slit. The 1D rms residuals over each of the 9 sectors are given in Table 5 For LRIS-R, the maximum rms difference in X for any sector in any of the images listed (see table below) is only 0.14 arcsec, and this high value is achieved only in sectors 3 and 7, which are two of the four outer corners (the corner sectors are 1, 3, 7 and 9). Thus for purposes of slitmask design, maximum uncertainties of 0.14 arcsec will occur if you try to use the full LRIS imaging area, and maximum errors of 0.10 arcsec[1] will occur if you use only the central 1/3 of the detector in X over the full height of the CCD. Errors of 0.1 arcsec (corresponding to 0.47 pixels for LRIS-R, which is 11μ in the instrument focal plane) surely can be tolerated within the area covered by objects to be assigned to a slitlet given that a typical width of each slitlet in a slitmask is 0.8 to 1.0 arcsec.

A comparison of Fig. 2 with 3 (ADC in and ADC out, applying distortion fits to the same frame from which they were derived) shows that the stars with larger deviations in the central region of the image are the same in both figures. This suggests that errors in the J2000 positions, presumably from proper motions differing from those of the bulk of the open cluster stars, are probably causing these deviations.

[1]One relevant entry in Table 5 is 0.11 arcsec.

Most of these small residuals must arise from uncertainties in the input RA,Dec for the sample of stars. There may be additional contributions from differential thermal effects on the various nights during which data was obtained. Another possibility could be the distortion arising in the optical system before the camera. Our calculated correction is assumed to be fixed with the CCD irrespective of how the field ratates during observation. But there are many optical components in the opitical path that are not fixed to the CCD, including any distortion from the telescope optics.

We can examine the effect of the use of different filters from the above table. There is no detectable difference in the fits between frames taken with the V and with the R filters.

Table 3. Position Angles of LRIS-R Images

Frame	Field	Date	ADC	PA[a] (deg)	ΔPA[b] (deg)
0040	NGC2158	2007/01/28	Yes	90.0	−0.07
0041	NGC2158	2007/01/28	Yes	90.0	0.07
0052	Leo I	2007/01/28	Yes	110.0	0.08
0070	NGC2158	2007/02/16	No	90.0	−0.07
0102	Leo I	2007/03/09	Yes	110.0	0.10
0250	Leo I	2006/12/29	No	110.0	−0.91

[a]This is 90° + the keyword value of ROTPOSN.

[b]PA inferred from astrometric solution – (90° + PA from keyword ROTPOSN), with value of ROTPOSN taken from header of FITS image.

Image	Template	Filter	ADC	σ_r(S1)	σ_r(S2)	σ_r(S3)	σ_r(S4)	σ_r(S5)	σ_r(S6)	σ_r(S7)	σ_r(S8)	σ_r(S9)
0040	0040	R	Y	0.09	0.08	0.08	0.07	0.07	0.08	0.08	0.08	0.09
0041	0040	V	Y	0.13	0.11	0.13	0.10	0.08	0.10	0.14	0.12	0.11
0052	0040	R	Y	0.12	0.09	0.19	0.08	0.09	0.06	0.07	0.13	0.23
0102	0040	R	Y	0.05	0.07	0.09	0.07	0.07	0.12	0.20	0.10	0.08
0070	0070	R	N	0.08	0.08	0.08	0.07	0.08	0.08	0.08	0.07	0.10
0071	0070	R	N	0.10	0.08	0.07	0.07	0.08	0.08	0.08	0.08	0.09
0250	0070	R	N	0.24	0.14	0.19	0.16	0.08	0.12	0.08	0.20	0.30
0055	0055	G	Y	0.08	0.08	0.08	0.08	0.07	0.07	0.08	0.07	0.08
0056	0055	B	Y	0.09	0.09	0.09	0.08	0.08	0.07	0.12	0.08	0.08
0162	0055	G	Y	0.23	0.07	0.07	0.12	0.09	0.08	0.08	0.11	0.08
0096	0055	B	Y	0.12	0.09	0.13	0.14	0.09	0.11	0.19	0.06	0.08
0062	0062	B	N	0.08	0.07	0.08	0.08	0.08	0.08	0.08	0.08	0.08
0063	0062	B	N	0.10	0.08	0.08	0.08	0.08	0.09	0.09	0.08	0.08
0205	0062	B	N	0.15	0.16	0.16	0.08	0.10	0.08	0.24	0.14	0.16

Table 4: 2D Residuals for each sector of LRIS-R Images

Image	Template	Filter	ADC	σ_x(S1)	σ_x(S2)	σ_x(S3)	σ_x(S4)	σ_x(S5)	σ_x(S6)	σ_x(S7)	σ_x(S8)	σ_x(S9)
0040	0040	R	Y	0.06	0.05	0.06	0.04	0.05	0.06	0.06	0.06	0.07
0041	0040	V	Y	0.08	0.06	0.07	0.07	0.06	0.07	0.09	0.06	0.07
0052	0040	R	Y	0.09	0.05	0.11	0.08	0.07	0.03	0.05	0.07	0.12
0102	0040	R	Y	0.03	0.03	0.07	0.06	0.03	0.11	0.14	0.08	0.07
0070	0070	R	N	0.06	0.05	0.06	0.05	0.05	0.06	0.06	0.05	0.08
0071	0070	R	N	0.07	0.05	0.05	0.05	0.06	0.05	0.06	0.05	0.06
0250	0070	R	N	0.05	0.04	0.14	0.09	0.03	0.03	0.06	0.06	0.06
0055	0055	G	Y	0.06	0.06	0.05	0.06	0.05	0.05	0.05	0.06	0.06
0056	0055	B	Y	0.06	0.06	0.06	0.06	0.05	0.05	0.06	0.06	0.06
0162	0055	G	Y	0.12	0.03	0.05	0.04	0.04	0.03	0.03	0.03	0.02
0096	0055	B	Y	0.04	0.03	0.07	0.10	0.04	0.08	0.14	0.05	0.07
0062	0062	B	N	0.06	0.06	0.05	0.06	0.05	0.06	0.05	0.06	0.06
0063	0062	B	N	0.08	0.06	0.06	0.07	0.06	0.07	0.06	0.06	0.06
0205	0062	B	N	0.15	0.14	0.15	0.07	0.05	0.03	0.23	0.13	0.06

Table 5: 1D Residuals for each sector in the X Direction of LRIS-R Images

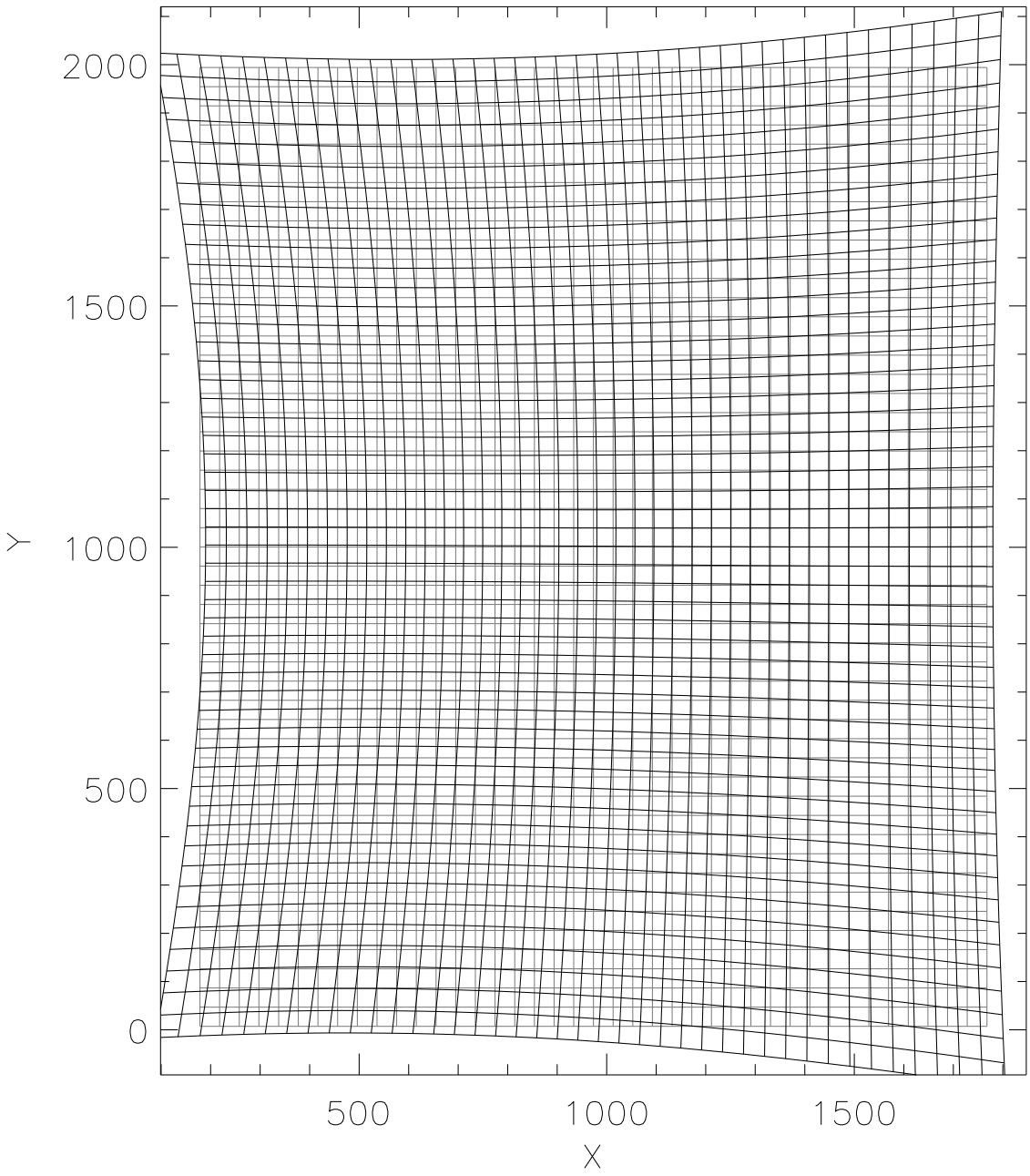

Fig. 1.— The distortion pattern of the LRIS-R optics is illustrated (from lred0040). The residuals from a linear fit are shown magnified by a factor of 15.

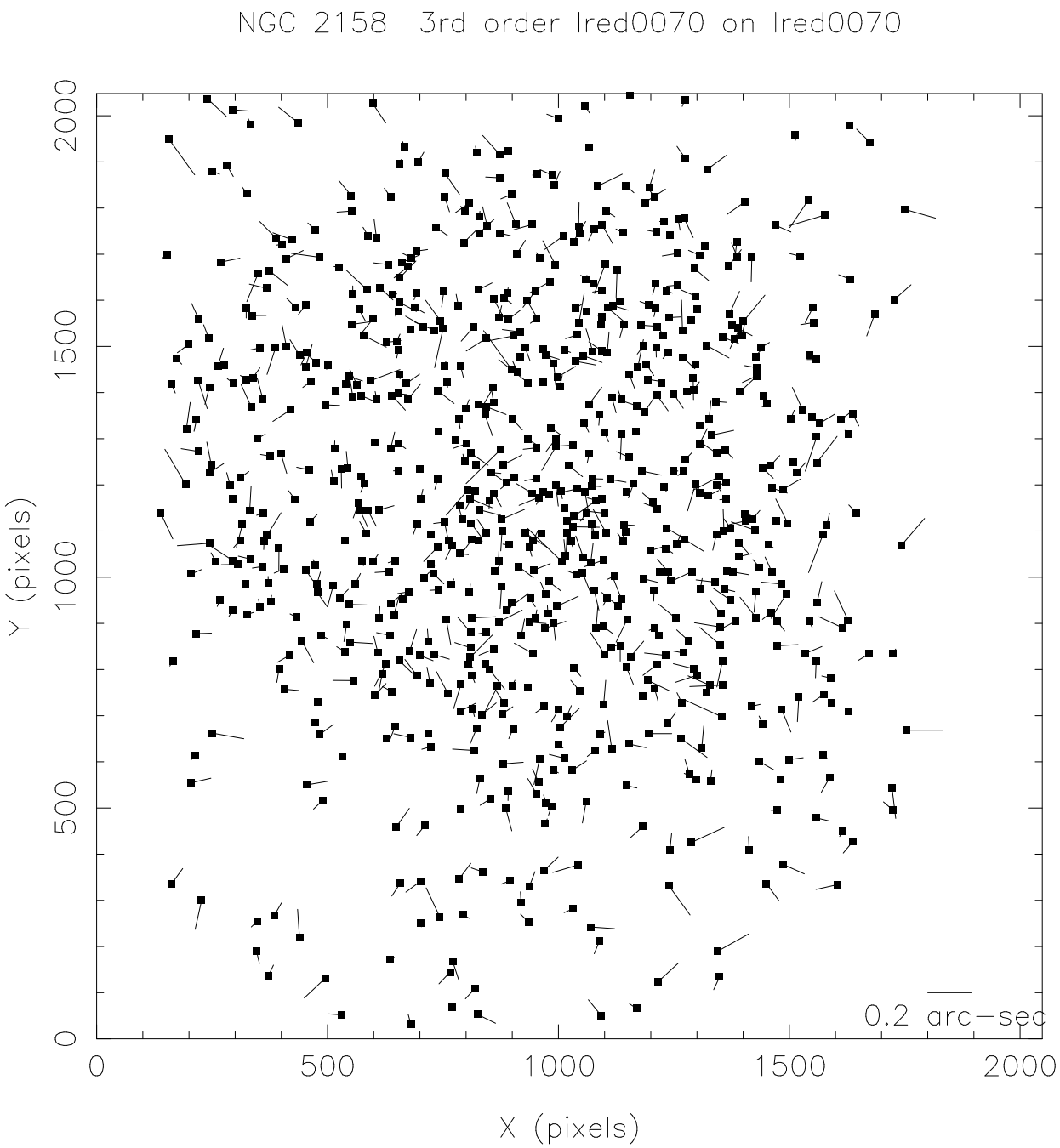

Fig. 2.— The "true" positions (astrometry data) for ∼730 stars in the field of the open cluster NGC 2158 are plotted as diamonds. The distortion fit and the image analyzed are both lred0070. The ADC was not in use for this image. The bars show the residuals of the positions calculated from the distortion fit. The residuals are shown magnified by a factor of 100.

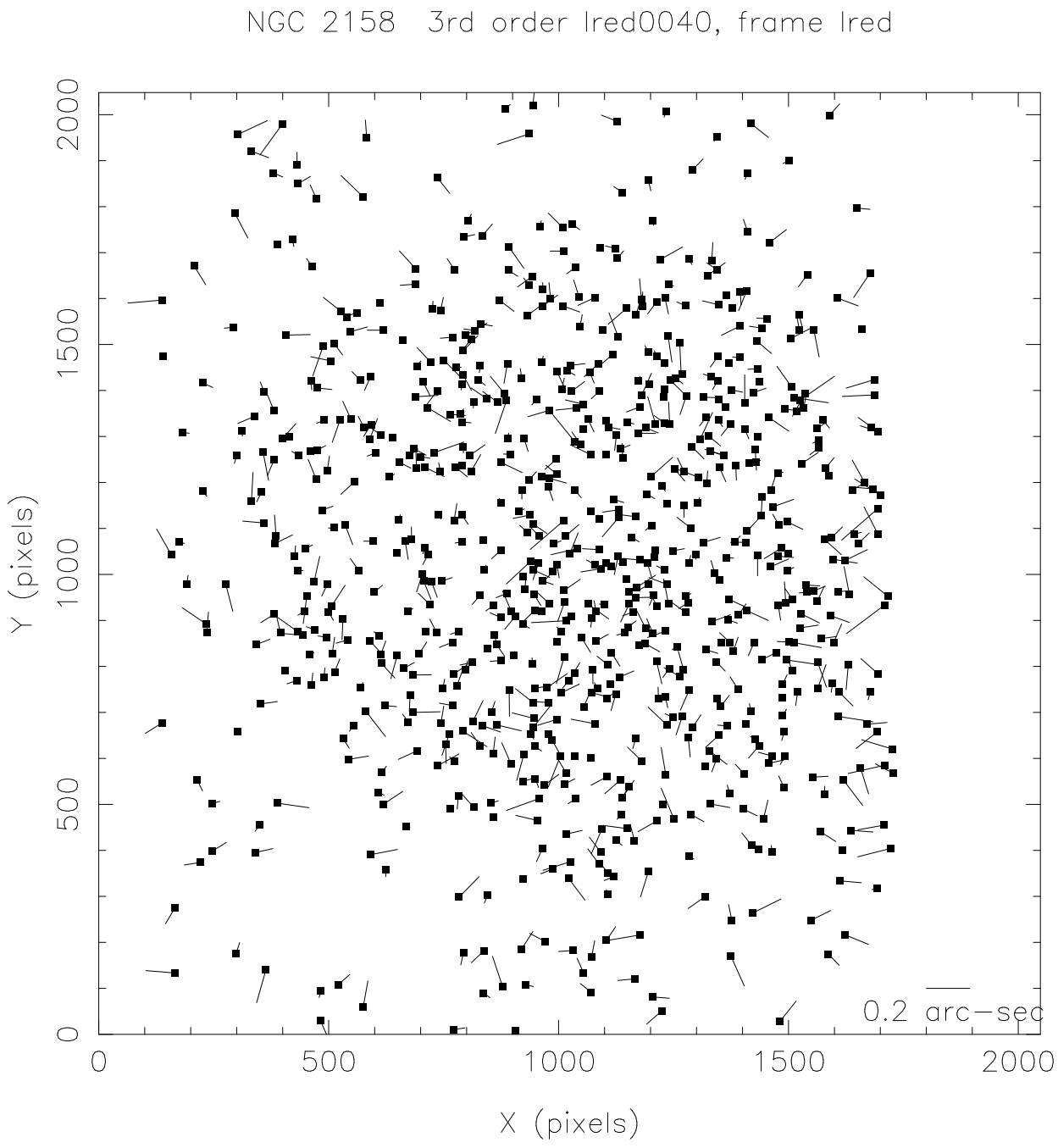

Fig. 3.— The "true" positions (astrometry data) for ∼730 stars in the field of NGC 2158 are shown. The distortion fit and the image analyzed are both lred0040. The ADC was in use. The short lines show the residuals of the positions calculated from the distortion fit. The residuals are magnified by a factor of 100.

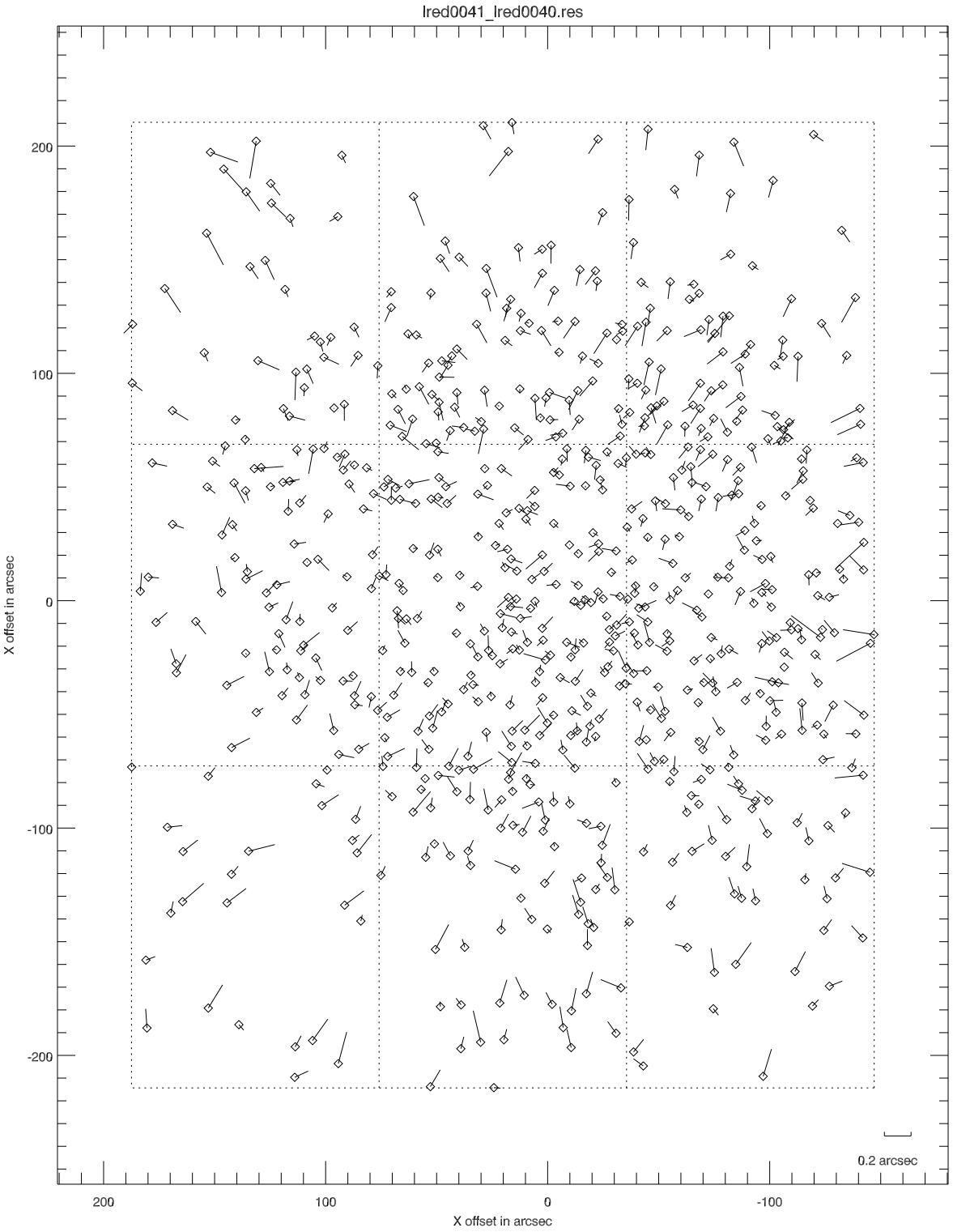

Fig. 4.— The "true" positions (astrometry data) for ∼730 stars in the field of NGC 2158 are shown. The distortion fit is from lred0040 and the image analyzed is lred0041. The ADC was in use. The short lines show the residuals of the positions calculated from the distortion fit. The residuals are magnified by a factor of 60.

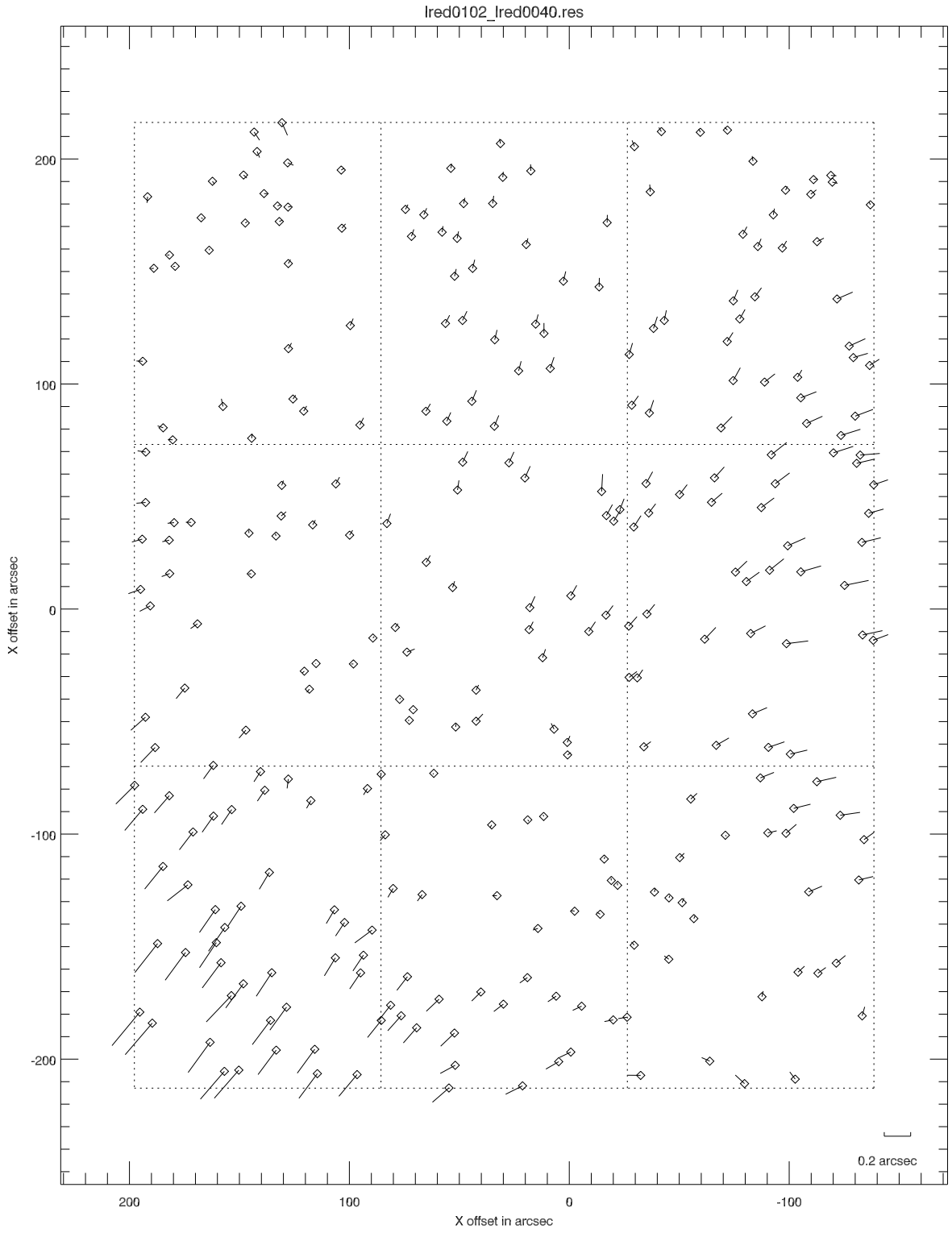

Fig. 5.— The "true" positions (astrometry data) for ∼290 stars in the field of the Leo I dwarf galaxy are plotted as diamonds. The distortion fit is from lred0040 and the image analyzed is lred0102. These frames were taken 1.5 months apart. The ADC was in use. The bars show the residuals of the positions calculated from the distortion fit. The residuals are magnified by a factor of 60.

5. The Blue Camera: LRIS–B

The detector on the blue side of LRIS is a mosaic of two CCDs whose format is described above. The mosaic is permanently mounted and is never adjusted, at least not since its initial installation. Fig. 7 is a sketch of the LRIS–B detector mosaic. The size of the pixels in this detector is 15μ, significantly smaller than those in the LRIS–R detector.

There is a gap between the two CCDs in this mosaic of 100 pixels in X; objects which fall within this gap are not imaged and this dead area is not part of the LRIS-B final image. There is a small shift in Y as well of -2.5 ± 1 pixels. The two CCDs are also slightly tilted with respect to each other by 0.09° deg.

Pixels with $X > 2252$, i.e. points falling on the right CCD of a LRIS-B image, must be rotated about the center of the right CCD and shifted appropriately, producing $X_{\rm final}$ and $Y_{\rm final}$, before calculating the astrometric fit. For $X_{\rm msr}$ and $Y_{\rm msr}$ being the pixel values as measured using the ds9 cursor, three steps (a shift, a rotation, and a second shift of opposite sign to the first one and also taking into account the gap) are necessary to get $X_{\rm final}, Y_{\rm final}$. The adopted relations are:

▶ for all pixels with $X_{\rm msr} \leq 2252$ (i. e. on the left chip),

$$X_{\rm final} = X_{\rm msr}, \quad Y_{\rm final} = Y_{\rm msr};$$

▶ for all pixels with $X_{\rm msr} > 2252$ (i. e. on the right chip),

$$\Delta X = X_{\rm msr} - 3100, \quad \Delta Y = Y_{\rm msr} - 2125,$$

$$\Delta X' = \Delta X \cos(\theta) - \Delta Y \sin(\theta), \quad \Delta Y' = \Delta X \sin(\theta) + \Delta Y \cos(\theta),$$

$$X_{\rm final} \ = \ \Delta X' + 3100 + 99.92, \quad Y_{\rm final} \ = \ \Delta Y' + 2125 - 4.43,$$

Here we adopt $\theta = -0.092°$, the mean of the analysis for all the NGC 2158 LRIS-B images in hand.

The equations have constants appropriate for X, Y(CCD) inputs from ds9; the equations found within the code for program COORDINATES assume the prepix pixels have been removed, so the constants are different.

The code assumes a four amplifier readout (two amps/CCD) for the mosaic CCD detetor used with LRIS-B. The prepix value for each amp is taken from the image header; the current value is 51 pixels/amplifier.

We follow an analysis similar to that used for LRIS-R, with the additional complication of implementing the transformation equations given above to adjust the measured

$X, Y(CCD)$ on the right side of the image. We adopt $X_{\rm final}, Y_{\rm final} = 2098, 2048$ as the center of rotation of LRIS-B images. (This is the size of each of the two CCDs in the mosaic plus half of the size of the gap between them.) We recall that the rotation required to achieve PA = 0° is 90° different for the LRIS-B as compared to LRIS-R. We carry out the same third order 10 parameter fit procedure as was described above using the images listed in Table 1. The deduced coefficients from lblue0055, taken with the ADC in use, and lblue0062, with the ADC out of the optical path, are given below.

The derived position angles of the LRIS-B frames analyzed here are given in Table 7. This table should be compared with the comparable table for LRIS-R, Table 3. The comparison suggests that the CCD mosaic in the blue camera of LRIS is slightly rotated (or some element in the camera itself is introducing a small rotation) with respect to LRIS-R by ∼0.4°. This issue is discussed further in §6.3.

Furthermore, comparison of these two tables, Table 3 and Table 7, shows the same problem for lblue0205 as was found for the matching LRIS-R frame, lred0250. The position angle for this pair of images, and only these two images, as determined from the instrument rotator and the telescope DCS differs from that found by analyzing the reference stars on the image by 0.9°. None of the other LRIS-R images shows a difference larger than 0.1°.

X/Y	ADC	1	x	y	x^2
		y^2	xy	x^3	x^2y
		xy^2	y^3		
lblue0055					
X	Yes	−274.83492	−0.10693314E−02	0.13192481	0.24581167E−06
		0.12822328E−05	0.84859900E−06	−0.43086048E−11	−0.19709703E−09
		−0.35997436E−11	−0.15949522E−09		
Y	Yes	−279.76069	0.13151461	−0.22063626E−02	0.12483489E−05
		0.25379359E−06	0.11612311E−05	−0.19916774E−09	−0.53179088E−12
		−0.16899998E−09	0.14019297E−10		
lblue0062					
X	No	−274.42599	−0.12496566E−02	0.13181624	0.32606807E−06
		0.12004263E−05	0.87444933E−06	−0.10594879E−10	−0.20943796E−09
		0.21221213E−11	−0.14837532E−09		
Y	No	−278.70945	0.13102987	−0.26848773E−02	0.12898216E−05
		0.40423847E−06	0.13085340E−05	−0.20381190E−09	−0.12707996E−11
		−0.20420376E−09	0.65189775E−12		

Table 6: Coefficients for LRIS-B (Third Order Polynomial Fit)

Table 7. Position Angles of LRIS-B Images

Frame	Field	Date	ADC	PA[a] (deg)	ΔPA[b] (deg)
0055	NGC2158	2007/01/28	Yes	0.0	0.38
0056	NGC2158	2007/01/28	Yes	0.0	0.39
0062	NGC2158	2007/02/16	No	0.0	0.39
0096	Leo I	2007/01/28	Yes	20.0	0.39
0162	Leo I	2007/03/09	Yes	20.0	0.41
0205	Leo I	2006/12/29	No	20.0	−0.60

[a]This is 90° + the keyword value of ROTPOSN.

[b]PA inferred from astrometric solution – (90° + PA from keyword ROTPOSN), with value of ROTPOSN taken from header of FITS image.

Image	Template	Filter	ADC	σ_r(S1)	σ_r(S2)	σ_r(S3)	σ_r(S4)	σ_r(S5)	σ_r(S6)	σ_r(S7)	σ_r(S8)	σ_r(S9)
0055	0055	G	Y	0.08	0.08	0.08	0.08	0.07	0.07	0.08	0.07	0.08
0056	0055	B	Y	0.09	0.09	0.09	0.08	0.08	0.07	0.12	0.08	0.08
0162	0055	G	Y	0.23	0.07	0.07	0.12	0.09	0.08	0.08	0.11	0.08
0096	0055	B	Y	0.12	0.09	0.13	0.14	0.09	0.11	0.19	0.06	0.08
0062	0062	B	N	0.08	0.07	0.08	0.08	0.08	0.08	0.08	0.08	0.08
0063	0062	B	N	0.10	0.08	0.08	0.08	0.08	0.09	0.09	0.08	0.09
0205	0062	B	N	0.15	0.16	0.16	0.08	0.10	0.08	0.24	0.14	0.16

Table 8: 2D Residuals for each sector of LRIS-B Images

Image	Template	Filter	ADC	σ_y(S1)	σ_y(S2)	σ_y(S3)	σ_y(S4)	σ_y(S5)	σ_y(S6)	σ_y(S7)	σ_y(S8)	σ_y(S9)
0055	0055	G	Y	0.06	0.04	0.06	0.05	0.05	0.05	0.06	0.05	0.05
0056	0055	B	Y	0.06	0.06	0.07	0.05	0.06	0.05	0.11	0.06	0.06
0162	0055	G	Y	0.15	0.06	0.04	0.07	0.08	0.05	0.05	0.11	0.05
0096	0055	B	Y	0.08	0.08	0.07	0.06	0.08	0.05	0.09	0.04	0.06
0062	0062	B	N	0.05	0.05	0.06	0.05	0.05	0.05	0.06	0.06	0.06
0063	0062	B	N	0.06	0.05	0.06	0.05	0.05	0.05	0.06	0.05	0.06
0205	0062	B	N	0.10	0.08	0.08	0.09	0.09	0.06	0.12	0.05	0.07

Table 9: 1D Residuals for each sector in the Y Direction of LRIS-B Images

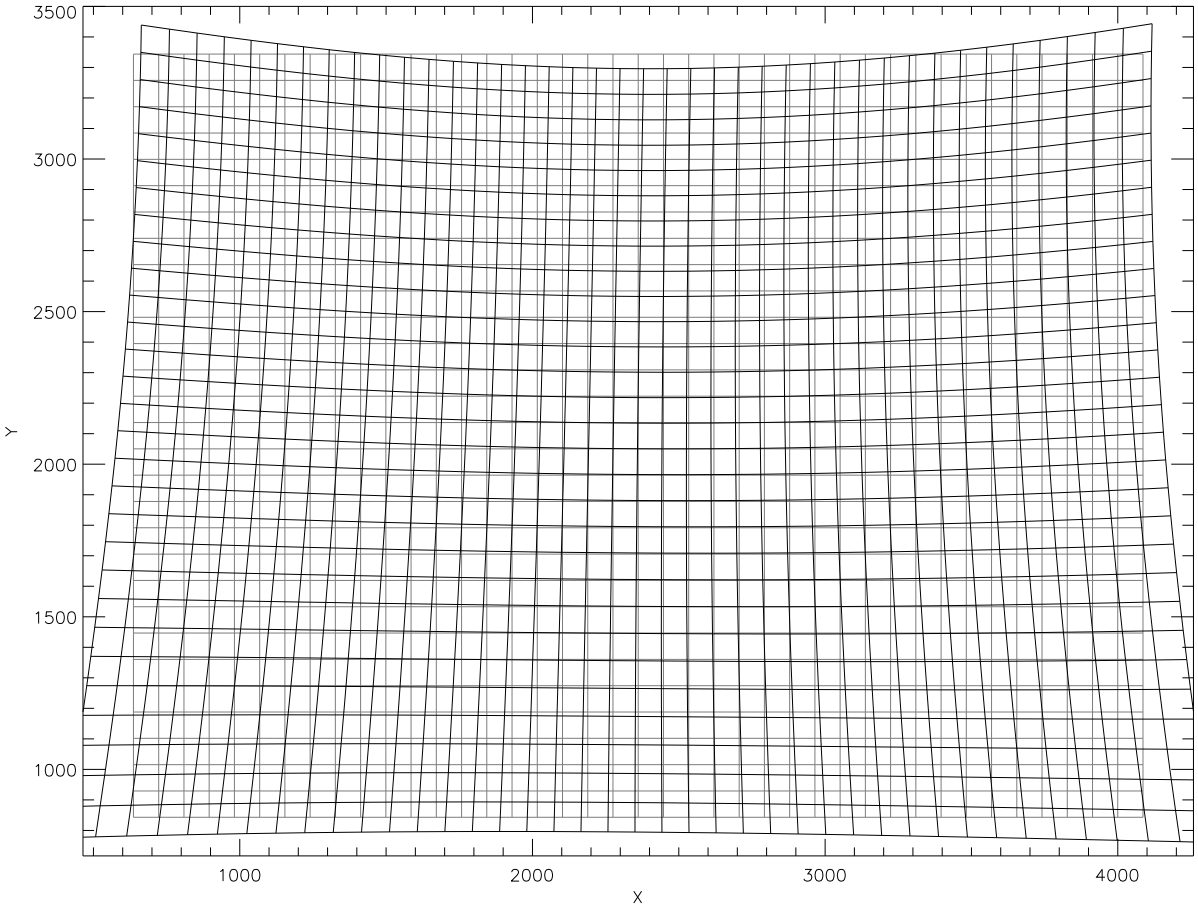

Fig. 6.— The distortion pattern of the LRIS-B optics is illustrated (from image lblue0062). The residuals from a linear fit are magnified by a factor of 15.

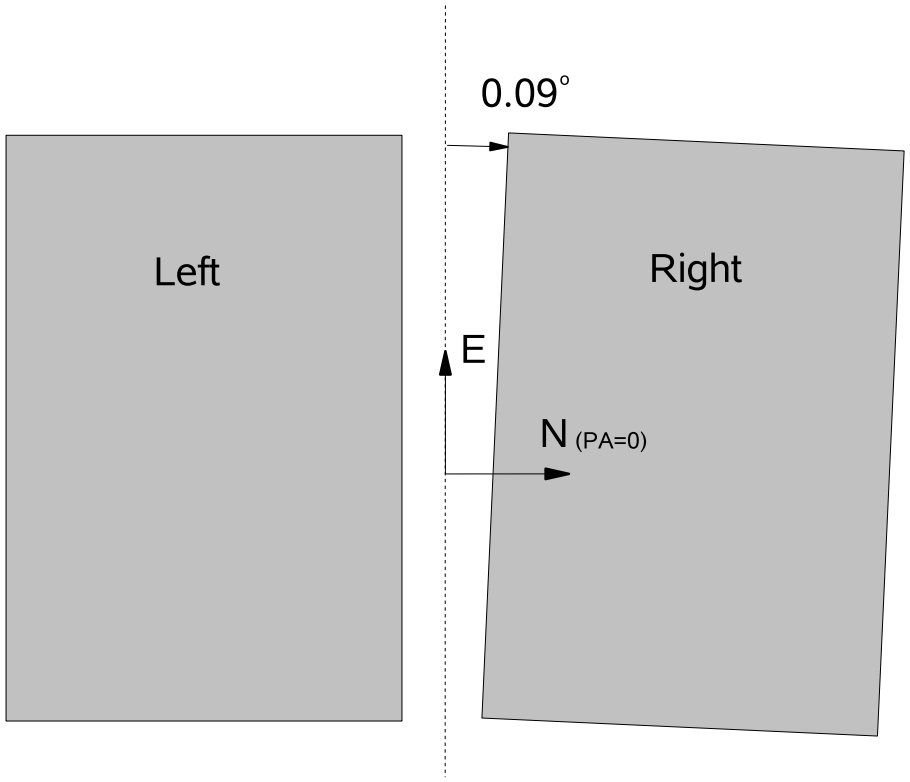

Fig. 7.— A sketch of the two CCD mosaic detector of LRIS–B. Note the slight tilt and the gap between the two CCDs. The orientation of N and E is illustrated for the nominal PA of 0°.

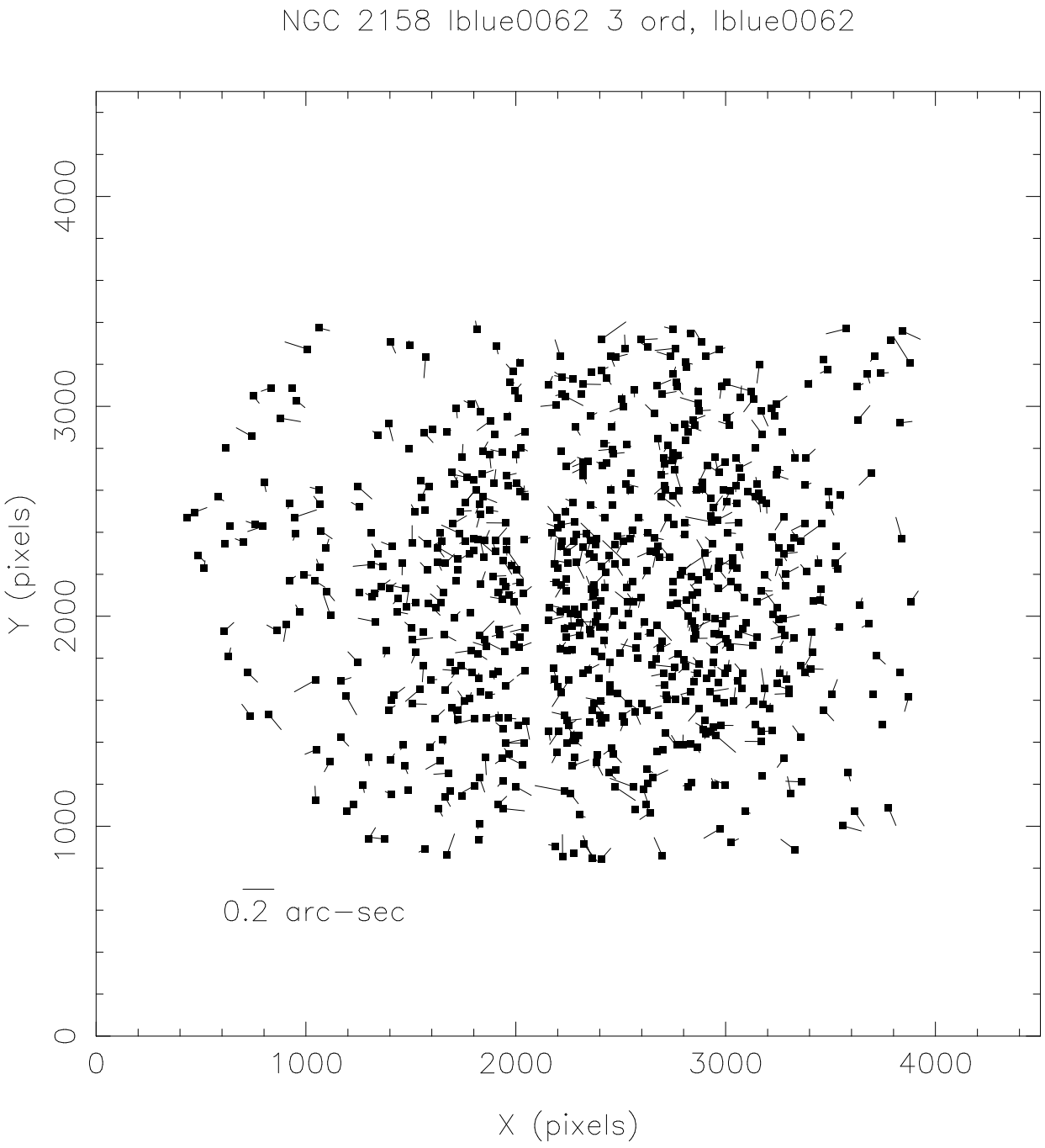

Fig. 8.— The "true" positions (astrometry data) for ∼730 stars in the field of NGC 2158 as seen in LRIS–B are shown. The distortion fit is derived from lblue0062 and is applied to that image. The ADC was not in use. The short lines show the residuals of the positions calculated from the distortion fit. The residuals are magnified by a factor of 100.

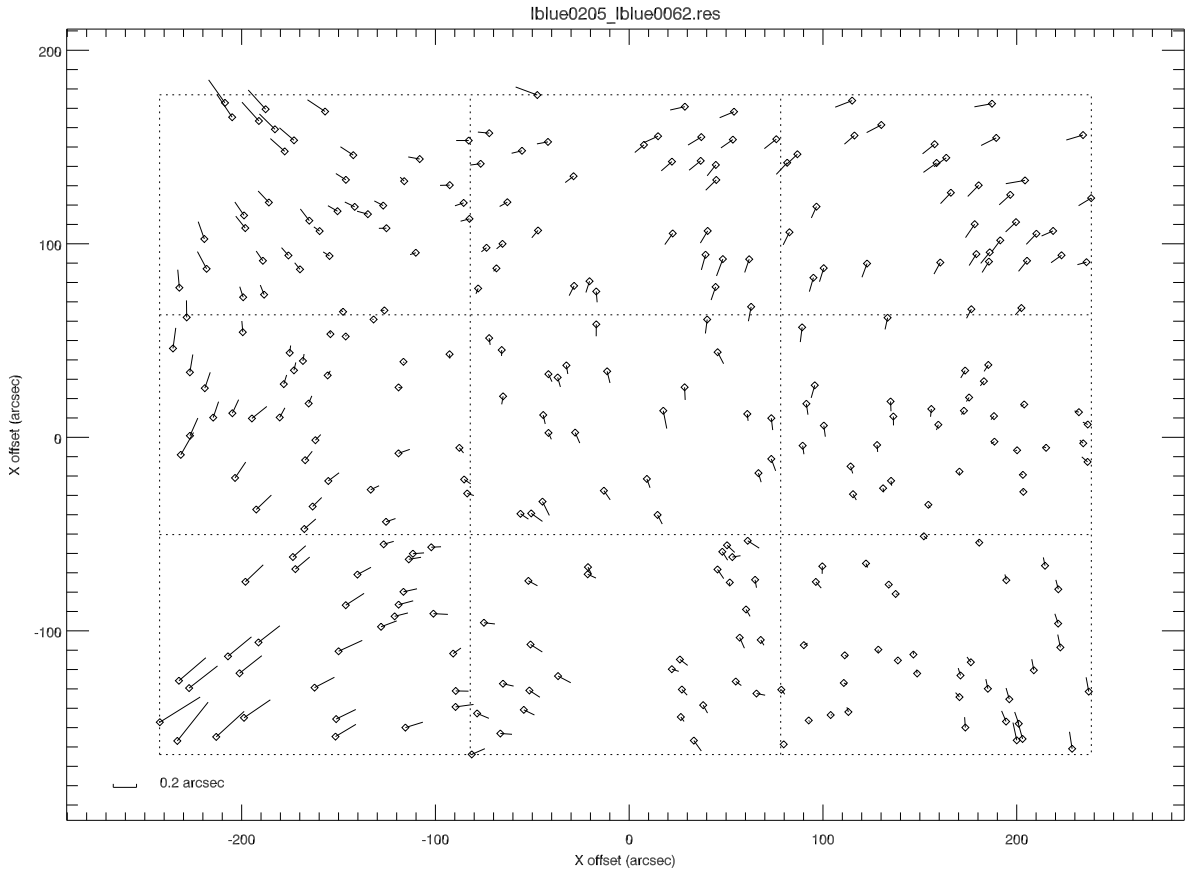

Fig. 9.— The "true" positions (astrometry data) for ∼730 stars in the field of NGC 2158 as seen in LRIS–B are plotted as diamonds. The distortion fit is derived from lblue0062 and is image lblue0205. The ADC was not in use. The bars show the residuals of the positions calculated from the distortion fit. The residuals are magnified by a factor of 60.

6. Important Warnings

6.1. History of Astrometric Fits to LRIS Detector Focal Plane

LRIS has had a series of detector upgrades and major instrument improvements since its original installation at Keck I in late 1993. J. Cohen carried out fairly regular astrometric monitoring from the original installation through to the dewar upgrade in 1996 (LRIS-R only at that time). But there was no systematic monitoring by J. Cohen (nor to her knowledge by the Keck staff or anyone else) between 1996 and the present. This means that there was no astrometric fit for LRIS-B between the time the new mosaic CCD detector was installed in late 2001 and the present. There is no reason to suspect that the astrometric properties of LRIS-B have changed since the installation of the upgraded mosaic two CCD detector. More seriously, no fit at all is available for LRIS-B frames taken with the original bluside 2048x2048 CCD, i.e. those taken between the date of installation of the blue side of LRIS into the instrument and the date of the detector upgrade.

Unfortunately during the installation of LRIS-B there were some unintended changes that had to be made to the LRIS-R dewar, shutter, etc. Although there may have been a small change in the astrometric properties of the LRIS focal plane after the installation of LRIS-B, there was no astrometric check to LRIS-R between that time (roughly late 2001) and the spring of 2007.

COORDINATES currently contains 4 sets of fits. The first two are for LRIS-R only, and represent the original dewar and the upgraded dewar installed in 1996. Then there are the two current fits for both red and blue LRIS cameras with and without the ADC in the beam.

The current fits for LRIS-B are used for all LRIS-B images taken after the CCD mosaic was installed in LRIS-B. No fit can be carried out for earlier LRIS-B frames. The current set of fits are used for all LRIS-R images taken after 2006.0, while the 1996 fits are used for LRIS-R images taken between 1996.5 and 2006.0.

6.2. ADC Issues

At the present time (August 3, 2007) it is impossible to tell from the keywords in the headers of LRIS images whether or not the ADC is in use. Until the LRIS software is modified appropriately by Keck personnel so that the ADC position is contained in the FITS header the user will have to indicate whether or not the ADC is used in the COORDINATES input file. The default, if this is not done, is to assume that that the ADC was used for all frames

taken after the installation of the ADC.

Once Keck personnel implement a way to determine the ADC status via FITS image header keywords, Version 3.1 will become available and will accomodate this new, as yet non-existent, feature.

Note that if the ADC is in the beam, even if it is not in use (i.e. the prisms are not rotating), perhaps to due mechanical problems, the astrometric fit must be that for when the ADC is in use.

6.3. Position Angle Issues

Position angle discrepancies Δ(PA) between the PA as determined from the positions of stars on the LRIS image and that of the instrument rotator on the Keck I Telescope will occur if the Dewar rotation on either the red or blue side of LRIS is not correctly aligned so that the central column in the red side detector (central row on the LRIS-B CCD mosaic) is parallel to the Dec axis when the commanded position angle is 0.0°. In the past, this alignment for LRIS-R was generally correct such that $-0.15 < \Delta(PA) < 0.15°$. Mechanical or electronic problems with the LRIS instrument rotator can also give rise to position angle discrepancies.

The position angle discrepancies found in the current test images for LRIS-R are discussed in §4 and listed in Table 3. They are small for all the LRIS-R images studied here except for the frame lred0250, where $\Delta(PA) = 0.9°$. Those for the matching LRIS-B exposures are about 0.4°, except for lblue0205, the matching frame to lred0250, which has a PA discrepancy 1.0° different from the other LRIS-B images.

We presume that the approximately constant typical $\Delta(PA)$ for LRIS-B images of 0.4° arises from a mis-alignment of the rotation of the LRIS-B dewar.

A $\Delta(PA)$ of 0.15° will cause an error in the output position inferred from the program COORDINATES of an object which is located in the extreme corner of the LRIS imaging field of ∼0.6 arcsec. To avoid such errors, the current version of the program COORDINATES has an option to determine the position angle directly from the reference stars with known astrometric coordinates detected on a LRIS image.

Please report any cases of large apparent $\Delta(PA)$ (i.e. $\mid \Delta(PA) \mid > 0.2°$) that occur on LRIS-R images to me and to appropriate Keck personnel.

Acknowledgements

We are grateful to A. Phillips, R. Ellis and G. Wirth for obtaining the test LRIS images used here.

file /home/gringo/jlc/lris/coordinates/april2007/report_spring2007.tex